Multiplicity distributions in $p\bar{p}$ collisions at 540 GeV and "bremsstrahlung analogy"

A. Bialas
Institute of Physics, Jagellonian University, Cracow, Poland

E. H. de Groot* and Th. W. Ruijgrok
Institute for Theoretical Physics, Rijksuniversiteit, Utrecht, The Netherlands†

(Received 3 July 1986)

Multiplicity distributions of particles produced in different rapidity intervals in 540-GeV $p\bar{p}$ collisions are analyzed using the model of "bremsstrahlung analogy." It is found that the model describes the main features of the data well, although the detailed shape of the distributions for large rapidity intervals is not precisely recovered. Fluctuations of the plateau height are described by a Γ distribution with $k=2$.

I. INTRODUCTION

In this paper, we analyze, using the model of "bremsstrahlung analogy,"[1,2] the new data on the multiplicity distribution of particles produced in $p\bar{p}$ collisions at 540 GeV (Ref. 3). It was shown in Ref. 3 that in all (pseudo) rapidity intervals $(-\eta_c,\eta_c)$ centered at $\eta=0$, the multiplicity distributions can be fitted very well by a negative-binomial distribution:

$$P(n)=\begin{bmatrix} n+k-1 \\ k-1 \end{bmatrix}\left[\frac{\langle n\rangle/k}{1+\langle n\rangle/k}\right]^n(1+\langle n\rangle/k)^{-k}, \tag{1.1}$$

where $\langle n\rangle$ is the average multiplicity. k is a parameter related to the relative width of the distribution $D/\langle n\rangle$ by the formula

$$k^{-1}=\left[\frac{D}{\langle n\rangle}\right]^2-\frac{1}{\langle n\rangle}. \tag{1.2}$$

It was found in Ref. 3 that k^{-1} (and, thus, also the relative width of the distribution) decreases with increasing η_c.

Let us also note that in the limit $\langle n\rangle\to\infty$, $\langle n\rangle P(n)$, i.e., the Koba-Nielsen-Olesen (KNO) function[4] of the distribution (1.1), tends to[5]

$$\langle n\rangle P(n)\to\psi(z)=\frac{k^k}{\Gamma(k)}z^{k-1}e^{-kz} \tag{1.3}$$

with $z=n/\langle n\rangle$. It was argued in Refs. 6 and 7 that the shrinking of the KNO function with increasing rapidity interval can be qualitatively understood as an effect of energy and momentum conservation which tends to cut the high-multiplicity tail of the distribution and which effects are clearly stronger for a large rapidity interval than in the central region where the produced particles are very slow. Using the model of bremsstrahlung analogy,[1,2] it was also shown that the size of this effect is substantial: it can approximately account for the observed violation of KNO scaling between CERN ISR and collider energies[6] and for the difference between the spectra in the central rapidity and full rapidity regions.[7]

In this paper we extend the analysis of Refs. 6 and 7 in two directions. First, we improve some approximations employed there: (a) we do not neglect the width of the elementary "bremsstrahlunglike" components and (b) we do take into account the effects of the decay of the produced clusters. We show, in fact, that these two effects introduce important quantitative corrections to the picture. Second, we compare the results with the recent data of Ref. 3 which are much more detailed and complete than the data of Ref. 8 which were analyzed in Ref. 6.

In the next section we describe the model of "bremsstrahlung analogy" for the production of particle clusters[1,2] and introduce some basic notation. In Sec. III the energy and momentum constraints are analyzed. Section IV deals with the effects of the cluster decay. Our conclusions are listed in the last section. In Appendix A some analytic formulas for the correlation coefficients in cluster production are derived while Appendix B gives the derivation of the corrections as a result of the decay of the clusters.

II. PARTICLE PRODUCTION AND "BREMSSTRAHLUNG ANALOGY"

In the bremsstrahlung analogy the multiproduction of particle clusters is taken to be a sum of simple components, each one giving a uniform distribution in rapidity y, $d\bar{n}/dy=\lambda$, and a Poissonian multiplicity distribution. This is very much like the situation in ordinary bremsstrahlung by a charged particle, where a given trajectory of the particle, corresponding to a certain classical current, produces one such simple Poissonian component. If we do not select the trajectory of the charged particle, however, we get a sum of the various simple components. We recall that this approach gives a general picture of the qualitative features of multiproduction, a correct description of leading-particle behavior,[1,2] and accurately predicted the forward-backward correlations found at the CERN collider.[9]

Each simple component is labeled by the density in ra-

pidity of the produced objects ("clusters"), and we call this density λ, which may be considered as analogous to the strength of the classical current or the strength of the coupling to the radiation field. The probability of having a certain λ in a collision is given by a weight function ψ. For future convenience and without loss of generality, we choose to write ψ as a function of $\lambda/\bar{\lambda}$. Thus,

$$\text{probability of } \lambda = \psi(\lambda/\bar{\lambda})\frac{1}{\bar{\lambda}}d\lambda \ . \tag{2.1}$$

With this normalization in addition to $\int \psi(z)dz = 1$, we also have $\int z\psi(z)dz = 1$. It was shown in Ref. 6 that in the high-energy limit $\psi(z)$ is identical to the asymptotic KNO function.[4]

Now the observed multiplicity distribution $P(N)$ is given by a weighted sum over the fundamental Poisson distributions $p(\lambda,N)$:

$$P(N) = \int p(\lambda,N)\psi(\lambda/\bar{\lambda})\frac{1}{\bar{\lambda}}d\lambda \ . \tag{2.2}$$

To summarize, the dynamical content of the model is characterized by (a) the independent emission of particle clusters and their subsequent decay and (b) the fluctuation of the plateau height λ as expressed by the function $\psi(\lambda/\bar{\lambda})$.

The physical origin of these fluctuations in λ is not entirely clear. One may think of them as a reflection of the dependence of particle production on the impact parameter[10] or on momentum transfer in elementary parton-parton scattering which presumably starts the observed process of particle production.[11] It should be stressed that, without further physical input, the model does not make any statements about the shape and energy dependence of $\psi(\lambda/\bar{\lambda})$. However, once $\psi(\lambda/\bar{\lambda})$ is known, the model gives well-defined predictions, which can be tested experimentally.

In the high-energy limit, when energy-conservation constraints are unimportant, $p(\lambda,N)$ is a Poisson distribution characterized by an average multiplicity $\bar{N}(\lambda)$ given by

$$\bar{N}(\lambda) = \lambda\,\Delta y \ , \tag{2.3}$$

where Δy is the rapidity interval considered.

Equation (2.3), when substituted into (2.2) with the scaling function given by (1.3), gives, after integration over λ, the multiplicity distribution of the produced *clusters* $P(N)$ in the form (1.1) with

$$\langle N \rangle = \bar{\lambda}\,\Delta y \ . \tag{2.4}$$

To obtain a realistic distribution of the produced *particles* one has to take into account two effects. First, energy- and momentum-conservation constraints should be introduced. Their effect is twofold: (a) they modify the shape of the distribution $p(\lambda,N)$ making it narrower than the original Poissonian distribution; and (b) they also modify the simple linear relation between $\bar{N}(\lambda)$ and λ. It was shown in Ref. 6 that the second effect has important consequences for the observed distribution of particles and can even explain an apparent violation of KNO scaling as observed by the UA5 Collaboration. These corrections, which both induce a shrinking of the distribution with respect to the nonconstrained distribution (1.1), are small in the central region of rapidity $\Delta y \ll Y_{\max}$ and become more important as Δy is closer to $Y_{\max}$. As a result, the KNO distribution shrinks when Δy increases toward $Y_{\max}$. This is in qualitative agreement with the results of the UA5 Collaboration.[3]

The second effect one has to consider is the decay of the clusters into particles. It is more important at small Δy where the number of particles is not very large.

We see that the two effects described above are largely complementary and both work in the direction required by the data: the KNO spectrum shrinks at large Δy. The question remains as to whether they are strong enough to explain the actually observed change in the data as the rapidity interval changes. This is analyzed in the next two sections.

III. CORRECTIONS FOR ENERGY AND MOMENTUM CONSERVATION

In this section we show how energy- and momentum-conservation constraints modify the cluster multiplicity and rapidity distributions. In view of the general formulas (2.2), we only need to know the effects of the conservation laws on the distribution $p(\lambda,N)$ which otherwise would be a simple Poissonian. In our approach, based on the "bremsstrahlung analogy,"[1,2] the distribution of clusters at fixed λ is given by the longitudinal-phase-space formula

$$\Omega_N = \frac{1}{N!}\prod_{i=1}^{N}\lambda\frac{dp_i}{\epsilon_i}\int dp_L dp_R\,\delta\left[P_0-\epsilon_L-\epsilon_R-\sum_{i=1}^{N}\epsilon_i\right] \times\delta\left[P-p_L-p_R-\sum_{i=1}^{N}p_i\right] ; \tag{3.1}$$

P_0 and P are the total energy and (longitudinal) momentum of the system, p_L, p_R are the momenta of the leading clusters, and $p_1 \cdots p_N$ are the momenta of the produced clusters. The corresponding energies are denoted by ϵ's. In Eq. (3.1) the transverse motion of the clusters is neglected (it contributes only to the transverse mass of the cluster).

The inclusive distributions of the produced clusters are then given by

$$\rho_M(\lambda;p_1,\ldots,p_M) = \lambda^M \sum_{N=0}^{\infty}\Omega_N(\lambda;P_0-\epsilon_1\cdots-\epsilon_M,P-p_1\cdots-p_M)\Big/\sum_{N=0}^{\infty}\Omega_N(\lambda;P_0,P) \ . \tag{3.2}$$

It was shown in Ref. 12 (cf. also Ref. 7) that

$$\sum_{N=0}^{\infty}\Omega_N(\lambda;Q_0,Q)\xrightarrow[Q_0^2-Q^2\to\infty]{\lambda\ \text{fixed}}\frac{1}{\Gamma(\lambda+1)^2}\left[\frac{e^{-2\gamma}}{m^2}\right]^{\lambda}(Q_0+Q)^{\lambda}(Q_0-Q)^{\lambda}\theta(Q_0+Q)\theta(Q_0-Q)\ , \tag{3.3}$$

$\gamma=0.5772\ldots$ Euler's constant .

Substituting (3.3) into (3.2) and introducing the light-cone variables $x_i^{\pm}=\mu e^{(y_i^{\pm})}$, where y_i are the rapidities of the produced clusters and

$$\mu=m/\sqrt{s} \tag{3.4}$$

(m is the transverse mass of the clusters), we obtain

$$\rho_M(\lambda;p_1,\ldots p_M)=\lambda^M(1-x_1^{+}-\cdots-x_M^{+})^{\lambda}(1-x_1^{-}-\cdots-x_M^{-})^{\lambda}\theta(1-x_1^{+}-\cdots-x_M^{+})\theta(1-x_1^{-}-\cdots-x_M^{-})\ . \tag{3.5}$$

This formula gives the inclusive distribution of the clusters taking the conservation laws into account. Our task now is to deduce from this the (exclusive) multiplicity distribution of the clusters in different intervals of rapidity. To this end we observe that the (factorial) moments of the cluster multiplicity distribution in the interval $-\eta_c$, η_c are given by

$$F_M(\lambda;\eta_c)=\int_{-\eta_c}^{\eta_c}\rho_M(\lambda;p_1,\ldots,p_M)dy_1\cdots dy_M\ , \tag{3.6}$$

in terms of which the distribution can be written as

$$P_N(\eta_c;\lambda)=\frac{1}{N!}\sum_{j=0}^{\infty}\frac{(-)^j}{j!}F_{N+j}(\lambda;\eta_c)\ .$$

By defining multiparticle correlation coefficients α_l by

$$F_k=(F_1)^k+\sum_{l=2}^{k}\binom{k}{l}\alpha_l(F_1)^{k-l}\ ,$$

one can show that

$$P_N(\eta_c;\lambda)=\frac{F_1{}^N e^{-F_1}}{N!}+\sum_{l=2}^{\infty}\frac{\alpha_l}{l!}\frac{d^l}{dF_1^l}\left[\frac{F_1{}^N e^{-F_1}}{N!}\right]\ , \tag{3.7}$$

hoping that the series converges rapidly, which should be the case if the corrections to a Poisson distribution are not too large. The l-particle correlation coefficients can be expressed in terms of factorial moments (3.6) (Ref. 13). For α_2 and α_3 we obtain

$$\alpha_2=F_2-F_1{}^2,\quad \alpha_3=F_3-3F_1F_2+2F_1{}^3\ . \tag{3.8}$$

In Fig. 1 the parameter $-\alpha_2/F_1$ is plotted versus λ for different values of η_c. In Fig. 2 the parameter $+\alpha_3/F_1$ is shown. One sees that these expansion parameters are small, particularly if η_c is not too close to $\eta_{\max}$. We conclude that, at this high energy, the expansion (3.7) is rapidly converging, and one can approximate the distributions by considering just one or two terms in (3.7).

The effects of the conservation laws on the width of the distribution can also be seen from Fig. 1 by observing that $\alpha_2/F_1=D^2/\langle n\rangle-1$. One sees that, as expected, the distribution is narrower than Poissonian (for Poissonian $D^2/\langle n\rangle=1$) and that the observed shrinking becomes important only when η_c is not far from $\eta_{\max}$.

Finally, in Fig. 3 we show the KNO plot for the cluster distribution $\langle N\rangle P_N$ integrated over λ according to the formula (2.2), using Eq. (1.3) with $k=2$, as suggested in Ref. 6. Other parameters were $\bar{\lambda}=1.55$ and cluster mass $=1$ GeV.

In performing this calculation $P_N(\eta_c;\lambda)$ was approximated by the first two terms in Eq. (3.7). Neglecting the non-Poissonian correction, $\alpha_2\neq 0$ hardly produces a change in the curves of Fig. 3. Only for $\eta_c=5.0$ the high-multiplicity tail of the distribution becomes slightly higher.

IV. EFFECTS OF THE CLUSTER DECAY

It is shown in Appendix B that the generating function for the distribution of particles in the interval $(-\eta_c,\eta_c)$

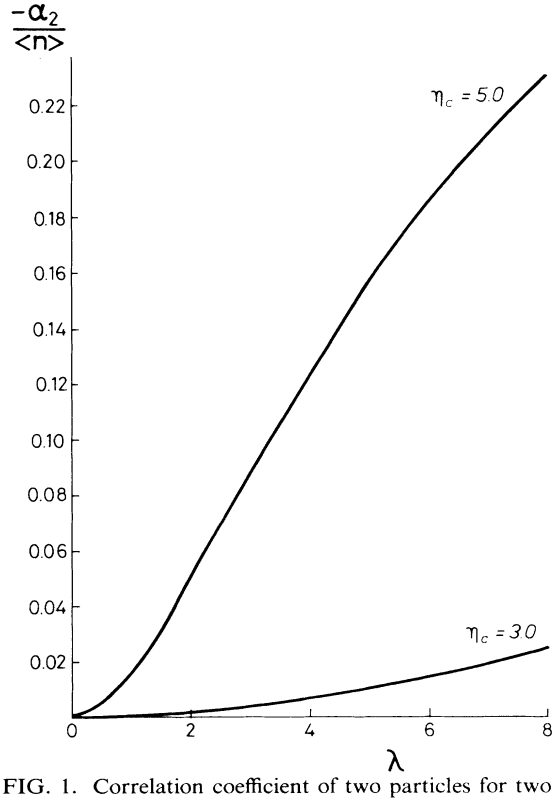

FIG. 1. Correlation coefficient of two particles for two values of the rapidity cutoff.

can be written as

$$\phi(z)=F[G(y;\eta_c;z)] , \tag{4.1}$$

where $F[\xi(y)]$ is the generating functional of the cluster rapidity distribution and $G(y;\eta_c;z)$ is the generating function of the distribution of particles in the interval $(-\eta_c,\eta_c)$ which come from the decay of a cluster produced at rapidity y.

Using the results of the previous section we write the generating functional $F[\xi(y)]$ in terms of the single-cluster inclusive distribution $\rho_1(y)$ and the two-cluster correlation function $C_2(y_1,y_2)$ as

$$F[\xi(y)]=\left[1+\tfrac{1}{2}\int dy_1 dy_2 C_2(y_1,y_2)\frac{\delta^2}{\delta\rho_1(y_1)\delta\rho_1(y_2)}\right]\exp\left[\int\rho_1(y)[\xi(y)-1]dy\right] , \tag{4.2}$$

where

$$C_2(y_1y_2)=\rho_2(y_1,y_2)-\rho_1(y_1)\rho_1(y_2) \tag{4.3}$$

with ρ_1 and ρ_2 given by Eq. (3.5).

For the rapidity distribution of the decay products of a cluster produced at rapidity y we assumed

$$D(y-y')dy'=\frac{1}{2}\frac{dy'}{\cosh^2(y-y')} . \tag{4.4}$$

If y and y' are pseudorapidities rather than rapidities, this distribution corresponds to isotropic decay of the clusters.

It follows from (4.4) that the probability that a particle from a cluster produced at rapidity y falls into the interval $(-\eta_c,\eta_c)$ is

$$d(y;\eta_c)=\int_{-\eta_c}^{\eta_c}D(y-y')dy'=\frac{\sinh 2\eta_c}{\cosh 2\eta_c+\cosh 2y} . \tag{4.5}$$

Consequently, the generating function $G(y,\eta_c;z)$ is

$$G(y,\eta_c;z)=g(1+d(y,\eta_c)(z-1)) , \tag{4.6}$$

where $g(z)$ is the generating function of the multiplicity distribution in the cluster decay. It was taken to be a polynomial in z. Assuming that the cluster can only decay into one, two, or three particles with respective probabilities α, $1-2\alpha$, and α, we get

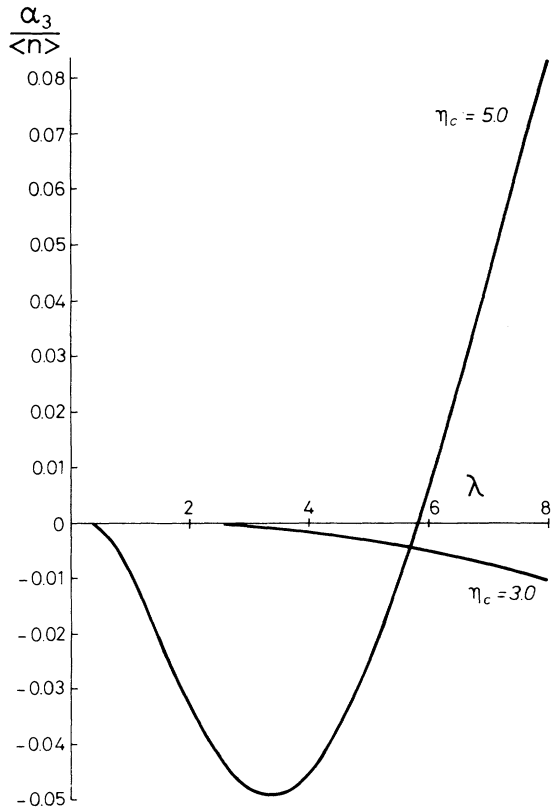

FIG. 2. Correlation coefficient of three particles for two values of the rapidity cutoff.

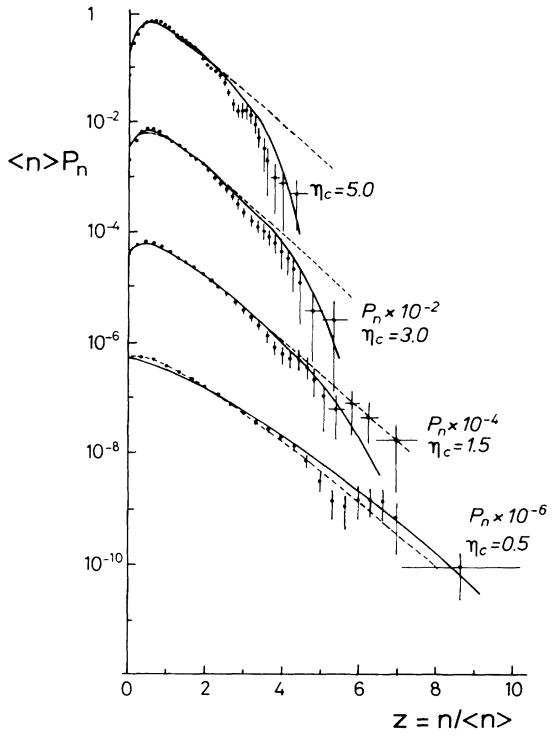

FIG. 3. KNO distribution of nondecaying clusters. The curves are calculated with $\bar{\lambda}=1.55$, $m=1$ GeV, and $\alpha_2\neq 0$. The dotted lines represent the distributions which are uncorrected for energy-momentum conservation. $\eta_{\max}=6.3$.

$$g(z)=\alpha z+(1-2\alpha)z^2+\alpha z^3 \ . \tag{4.7}$$

All calculations were performed for $\alpha=0.3$. The formulas (4.1)–(4.7) define the generating function of the particles in the interval $(-\eta_c,\eta_c)$. To obtain the distributions themselves we applied the relation

$$p(\lambda,n)=\frac{1}{n!}\frac{d^n\phi(z)}{dz^n}\bigg|_{z=0} \ . \tag{4.8}$$

The observed distribution of the particles in the interval $(-\eta_c,\eta_c)$ is obtained from $p(\lambda,n)$ by integrating over λ:

$$P(n)=\int \frac{d\lambda}{\bar{\lambda}}\psi\left[\frac{\lambda}{\bar{\lambda}}\right]p(\lambda,n) \ . \tag{4.9}$$

This formula gives the final distribution, which includes corrections from both energy-momentum conservation and cluster decay. In Fig. 4 the resulting KNO distributions $\langle n\rangle P(n)$ are plotted versus $n/\langle n\rangle$ for different values of η_c. For simplicity, they were calculated assuming $\alpha_2=0$. One sees a clear tendency of a broadening of the distribution with decreasing η_c. The experimental data from Ref. 3 are also shown in this figure. They are in reasonable agreement with our calculations. We conclude that our calculation reproduces the main features of the data. It is also seen, however, that some details of the distribution are not correctly described. Our calculation gives too high a value for the zero-prong probability and a slightly too long tail for $\eta_c=5$. On the other hand, it describes very well the general tendency of a shrinking of the distribution. We have checked that these features do not disappear when one varies the parameters of the cluster decay.

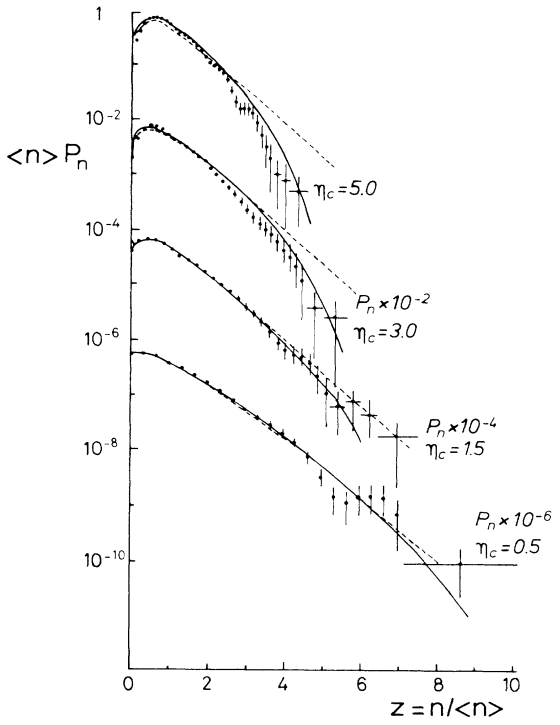

FIG. 4. KNO distribution of particles from clusters decaying into one, two, or three fragments; $\alpha_2=0$. Other parameters as in Fig. 3. The dotted lines are the same as in Fig. 3. $\eta_{\max}=6.3$.

V. CONCLUSIONS

We have analyzed the effects of energy and momentum conservation on the rapidity dependence of the multiplicity distribution of particles created in high-energy $p\bar{p}$ collisions.

Our conclusions can be formulated as follows.

(a) As already pointed out in Refs. 6 and 7, the effects of energy and momentum conservation are very strong, even at collider energies. They tend to make the KNO distribution in the larger rapidity intervals shrink significantly. This feature is qualitatively consistent with the data of Ref. 3.

(b) A realistic description of particle multiplicities, taking into account the presence of isotropically decaying clusters was attempted. Assuming the uncorrected distribution of clusters in the form of a negative binomial with $k=2$, it was shown that the combined effects of energy and momentum conservation and cluster decay provide a good description of the main features of the data.

(c) Some details of the data are not explained however: the calculated probability of zero-prong events is consistently too high, except at very small rapidity intervals; the tail of the calculated distribution is slightly too high compared to data at large rapidity intervals. We thus conclude that part of the dynamics is missing in the model. This is not surprising in view of its simplicity.

(d) The spectra obtained are not sensitive to details of the cluster decay.

To summarize, it was shown that a realistic model of bremsstrahlung analogy describes very reasonably the main features of the data on the multiplicity distribution as function of the rapidity. The remaining dynamical problem is therefore the origin of the cluster distribution in Eq. (1.3) with $k=2$. This problem remains, however, unsolved.

ACKNOWLEDGMENTS

One of the authors (A.B.) would like to thank A. Capella, F. Hayot, L. Stodolsky, and L. Van Hove for discussions. He is also grateful to the Laboratoire de Physique Théorique et Particules Elementaires at Orsay and to the Department of Theoretical Physics at Utrecht for their kind hospitality.

APPENDIX A: EFFECTS OF ENERGY-MOMENTUM CONSERVATION AT $\eta_c=Y_{\max}$

1. For fixed λ

We derive the deviation from a Poisson distribution [i.e., the α_l's from (3.7) and (3.8)] due to energy-momentum conservation in the case where we consider the full rapidity interval:

$$\eta_c = Y_{\max} = \tfrac{1}{2}\ln\frac{P\cdot P}{m^2} \ . \tag{A1}$$

All information can be obtained from (3.3):

$$C_\lambda \equiv \sum_N \Omega_N \simeq \left[\frac{P\cdot P}{m^2} e^{-2\gamma}\right]^\lambda \Gamma(\lambda+1)^{-2} \ , \tag{A2}$$

$\gamma = 0.5772\ldots$ Euler's constant .

We first create the generating function

$$G_\lambda(x) = \frac{C_{\lambda x}}{C_\lambda} = \sum_N x^N P_N \ , \tag{A3}$$

where the P_N's are the normalized multiplicity distributions

$$P_N = \frac{\Omega_N}{\Sigma_N \Omega_N} = \frac{1}{N!}\frac{d^N G_\lambda(x)}{dx^N}\bigg|_{x=0}$$

and where the factorial moments are given by

$$F_k(\lambda) = \langle N(N-1)\cdots(N-k+1)\rangle = \frac{d^k G_\lambda(x)}{dx^k}\bigg|_{x=1} \ . \tag{A4}$$

So, e.g.,

$$\langle N\rangle = 2\lambda[Y_{\max} - \gamma - \phi(\lambda+1)] \ ,$$

$$\phi(z) \equiv \frac{d\ln\Gamma(z)}{dz} \quad \text{digamma function} \ .$$

To better see the deviation from a Poisson distribution we write $G_\lambda(x)$ as

$$G_\lambda(x) = e^{2(Y_{\max}-\gamma)\lambda(x-1)}\left[\frac{\Gamma(\lambda+1)}{\Gamma(\lambda x+1)}\right]^2 = e^{\langle N\rangle(x-1)} e^{f_\lambda(x)} \tag{A5}$$

with

$$f_\lambda(x) \equiv 2\lambda(x-1)\psi(\lambda+1) + 2\ln\Gamma(\lambda+1) - 2\ln\Gamma(\lambda x+1) \ .$$

A Poisson distribution would have had $f_\lambda(x)=0$, so it comes as no surprise that we obtain, for the α_l's in (3.7),

$$\begin{aligned} &\alpha_l = \frac{d^l}{dx^l} e^{f_\lambda(x)}\bigg|_{x=1} \ , \\ &\alpha_0 = 1, \quad \alpha_1 = 0 \ , \\ &\alpha_2 = \langle N(N-1)\rangle - \langle N\rangle^2 = -2\lambda^2\phi'(\lambda+1) \ , \\ &\alpha_3 = -2\lambda^3\phi''(\lambda+1) \ , \\ &\alpha_4 = -2\lambda^4\phi''(\lambda+1) + 12\lambda^4[\phi'(\lambda+1)]^2, \text{ etc.} \ , \end{aligned} \tag{A6}$$

and thus

$$e^{f_\lambda(x)} = \sum_{l=0}^{\infty}\frac{\alpha_l}{l!}(x-1)^l \ . \tag{A7}$$

If we now break off this summation after the kth term we will still have the first k moments of the distribution correct, which gives an idea of how good an approximation it is to set, e.g., all $\alpha_3=\alpha_4=\cdots=0$, especially since after the integration over λ we will even have the first $k+1$ moments correct if we take $\alpha_{k+1}=\alpha_{k+2}=\cdots=0$. An improvement which is the result of the washing out of details due to the λ integration.

2. After integration over λ

We calculate the effect on the width of the KNO function due to energy and momentum conservation, after integrating over λ. This λ averaging will be indicated by additional angular brackets. We clearly have

$$\bar{F}_k = \langle\langle N(N-1)\cdots(N-k+1)\rangle\rangle = \int_0^\infty \psi\left[\frac{\lambda}{\bar{\lambda}}\right] F_k(\lambda)\frac{d\lambda}{\bar{\lambda}} \ . \tag{A8}$$

Substituting the $F_k(\lambda)$ from (A4) we have

$$\begin{aligned} &\langle\langle N\rangle\rangle = \int_0^\infty \frac{d\lambda}{\bar{\lambda}}\psi\left[\frac{\lambda}{\bar{\lambda}}\right] 2\lambda[Y_{\max} - \zeta'(\lambda)] \ , \\ &\langle\langle N(N-1)\rangle\rangle = \int_0^\infty \frac{d\lambda}{\bar{\lambda}}\psi\left[\frac{\lambda}{\bar{\lambda}}\right]\{4\lambda^2[Y_{\max} - \zeta(\lambda)]^2 - 2\lambda^2\zeta'(\lambda)\} \ , \end{aligned} \tag{A9}$$

where

$$\zeta(\lambda) \equiv \gamma + \phi(\lambda+1) \underset{\lambda\to\infty}{\sim} \gamma + \ln\lambda \ . \tag{A10}$$

In an obvious notation we then have, in first approximation,

$$\begin{aligned} &\langle\langle N\rangle\rangle = (2\bar{\lambda}Y_{\max} - 2\langle\lambda\zeta\rangle)\left[1 + 0\left[\frac{\langle\zeta\rangle}{Y_{\max}}\right]\right] \ , \\ &\langle\langle N(N-1)\rangle\rangle = (4\bar{\lambda}^2 Y_{\max}^2 - 8\bar{\lambda}\langle\lambda\zeta\rangle Y_{\max}) \times\left[1 + 0\left[\frac{\langle\zeta\rangle}{Y_{\max}}\right]\right] \ . \end{aligned} \tag{A11}$$

Therefore,

$$\frac{\langle\alpha_2\rangle}{\langle\langle N\rangle\rangle^2} = \frac{\langle\langle N(N-1)\rangle\rangle}{\langle\langle N\rangle\rangle} - 1 = \frac{\langle\lambda^2\rangle}{\bar{\lambda}^2}\frac{1 - 2\dfrac{\langle\lambda^2\zeta\rangle}{\langle\lambda^2\rangle}(Y_{\max})^{-1}}{1 - 2\dfrac{\langle\lambda\zeta\rangle}{\bar{\lambda}}(Y_{\max})^{-1}} \ . \tag{A12}$$

In general we will use only functions $\psi(\lambda/\bar{\lambda})$ for which $\bar{\lambda}\sim Y_{\max}$, so that we can replace ζ by

$$\zeta(\lambda) \sim \ln\lambda \quad (\lambda\to\infty) \ . \tag{A13}$$

We then obviously have

$$\langle\lambda^\alpha\zeta\rangle = \frac{\partial}{\partial\alpha}\langle\lambda^\alpha\rangle$$

and, thus,

$$\frac{\langle\lambda^\alpha\zeta\rangle}{\langle\lambda^\alpha\rangle} = \frac{\partial}{\partial\alpha}\ln\langle\lambda^\alpha\rangle \ . \tag{A14}$$

So we obtain, then,

$$\frac{\langle \alpha_2 \rangle}{\langle\langle N \rangle\rangle^2} = \frac{\langle \lambda^2 \rangle}{\bar{\lambda}^2} \left[1 - 2(Y_{\max})^{-1} \left[\frac{\partial \ln \langle \lambda^\alpha \rangle}{\partial \alpha} \bigg|_{\alpha=2} - \frac{\partial \ln \langle \lambda^\alpha \rangle}{\partial \alpha} \bigg|_{\alpha=1} \right] \right] - 1 \ . \tag{A15}$$

We now specify $\psi(z)$ to be of the form (1.3):

$$\psi(z) = \frac{k^2}{\Gamma(k)} e^{-kz} z^{k-1} \quad \text{for some } k > 0 \ . \tag{A16}$$

We then have

$$\langle \lambda^\alpha \rangle = \left[\frac{\bar{\lambda}}{k} \right]^\alpha \frac{\Gamma(\alpha + k)}{\Gamma(k)} \tag{A17}$$

and, thus,

$$\frac{\partial}{\partial \alpha} \ln \langle \lambda^\alpha \rangle \bigg|_{\alpha=2} - \frac{\partial}{\partial \alpha} \ln \langle \lambda^\alpha \rangle \bigg|_{\alpha=1} = \phi(k+2) - \phi(k+1) = \frac{1}{k+1} \tag{A18}$$

[ϕ is the digamma function of (A4)]. Inserting these results into (A15) one obtains

$$\frac{\langle \alpha_2 \rangle}{\langle \langle N \rangle \rangle^2} = \frac{2}{k} \left[\frac{1}{2} - \frac{1}{Y_{\max}} \right] , \tag{A19}$$

where $1/Y_{\max}$ is the result of energy-momentum conservation. Equation (A19) is also valid after the decay of the clusters into particles.

APPENDIX B: MULTIPLICITY DISTRIBUTION OF PARTICLES FROM DECAYING CLUSTER

Let us denote by $P_k(N_1, N_2, \ldots, N_k)$ the probability for producing N_1 clusters with rapidity between y_1 and $y_1 + \Delta$, N_2 clusters with rapidity between y_2 and $y_2 + \Delta$, etc., where $y_{m+1} = y_m + \Delta$. In the limit $\Delta \to 0$ ($k \to \infty$), the probability P_k gives a complete description of the cluster production. Thus information is conveniently summarized in the form of the generating functional defined as

$$F[\xi(\eta)] \equiv \lim_{k \to \infty} \sum_{N_1, \ldots, N_k} P_k(N_1, \ldots, N_k) [\xi(y_1)]^{N_1} \cdots [\xi(y_k)]^{N_k} \ . \tag{B1}$$

The distribution of clusters is recovered from $F[\xi(y)]$ by appropriate functional differentation.

If we now denote by $w_n(y; \eta_c)$ the probability distribution for n particles which originated from the decay of a cluster produced at rapidity y to be found in the interval $(-\eta_c, \eta_c)$, the distribution of particles in this interval is

$$P(n) = \lim_{k \to \infty} \sum_{N_1, \ldots, N_k} P_k(N_1, \ldots, N_k) \sum_{\substack{n_1^1 \cdots n_{N_k}^k \\ n_1^1 + \cdots n_{N_k}^k = n}} w_{n_1^1}(y_1, \eta_c) \cdots w_{n_{N_1}^1}(y_1; \eta_c) \cdots w_{n_1^k}(y_k, \eta_c) \cdots w_{n_{N_k}^k}(y_k, \eta_c) \ . \tag{B2}$$

The generating function of this distribution

$$\phi(z) \equiv \sum P(n) z^n \tag{B3}$$

is therefore

$$\begin{aligned} \phi(z) &= \lim_{k \to \infty} \sum_{N_1, \ldots, N_k} P_k(N_1, \ldots, N_k) \sum_{n_1^1 \cdots n_{N_k}^k} w_{n_1^1}(y_1, \eta_c) z^{n_1^1} \cdots w_{n_k^k}(y_n, \eta_c) z^{n_{N_k}^k} \\ &= \lim_{k \to \infty} \sum_{N_1, \ldots, N_k} P_k(N_1, \ldots, N_k) [G(y_1, \eta_c; z)]^{N_1} \cdots [G(y_k, \eta_c; z)]^{N_k} \ , \end{aligned} \tag{B4}$$

where we have denoted by $G(y, \eta_c; z)$ the generating function of the distribution $w_n(y, \eta_c)$. Comparing (B4) and (B1) one sees immediately that

$$\phi(z) = F[G(y, \eta_c; z)] \ . \tag{B5}$$

---

*On leave of absence from the University of Bielefeld, Federal Republic of Germany, GFR.

†Mailing address: Princetonplein 5, P.O. Box 80.006, 3508 TA Utrecht, The Netherlands.

[1] L. Stodolsky, Phys. Rev. Lett. **28**, 60 (1972); in *Proceedings of the VIIth Rencontre de Moriond*, edited by J. Tran Than Van (Editions Frontières, Marseilles, France, 1972), Vol. II.

[2] J. Benecke, A. Bialas, and E. H. de Groot, Phys. Lett **57B**, 447 (1975).

[3] UA5 Collaboration, G. J. Alner *et al.*, Phys. Lett. **167B**, 476

(1986).
[4]Z. Koba, H. B. Nielsen, and P. Olesen, Nucl. Phys. **B40**, 317 (1972).
[5]See, e.g., P. Carruthers and C. C. Shih, Phys. Lett. **127B**, 242 (1983).
[6]A. Bialas, I. Derado, and L. Stodolsky, Phys. Lett. **156B**, 421 (1985).
[7]A. Bialas and F. Hayot, Phys. Rev. D **33**, 39 (1986).
[8]UA5 Collaboration, G. J. Alner *et al.*, Phys. Lett. **138B**, 304 (1984).
[9]J. Benecke, A. Bialas, and S. Pokorski, Nucl. Phys. **B110**, 488 (1976); UA5 Collaboration, K. Alpgård *et al.*, Phys. Rev. Lett. **B123**, 361 (1983).
[10]See, e.g., S. Barshay, Phys. Lett. **42B**, 457 (1972); T. T. Chou and C. N. Yang, *ibid.* **116B**, 301 (1982).
[11]F. Low, Phys. Rev. D **12**, 163 (1975); S. Nussinov, Phys. Rev. Lett. **34**, 1286 (1975).
[12]E. H. de Groot, Nucl. Phys. **B48**, 295 (1972).
[13]See, e.g., M. G. Kendall and A. Stuart, *The Advanced Theory of Statistics* (Griffin, London, 1969), Vol. I, p. 163.